

# STIM2 protein mediates distinct store-dependent and store-independent modes of CRAC channel activation

Suhel Parvez,<sup>\*,1</sup> Andreas Beck,<sup>\*,1</sup> Christine Peinelt,<sup>\*</sup> Jonathan Soboloff,<sup>†</sup> Annette Lis,<sup>\*</sup> Mahealani Monteilh-Zoller,<sup>\*</sup> Donald L. Gill,<sup>†</sup> Andrea Fleig,<sup>\*</sup> and Reinhold Penner,<sup>\*,2</sup>

<sup>\*</sup>Center for Biomedical Research at The Queen's Medical Center and John A. Burns School of Medicine at the University of Hawaii, Honolulu, Hawaii, USA; and <sup>†</sup>Department of Biochemistry, School of Medicine, Temple University, Philadelphia, Pennsylvania, USA

**ABSTRACT** STIM1 and CRACM1 (or Orai1) are essential molecular components mediating store-operated Ca<sup>2+</sup> entry (SOCE) and Ca<sup>2+</sup> release-activated Ca<sup>2+</sup> (CRAC) currents. Although STIM1 acts as a luminal Ca<sup>2+</sup> sensor in the endoplasmic reticulum (ER), the function of STIM2 remains unclear. Here we reveal that STIM2 has two distinct modes of activating CRAC channels: a store-operated mode that is activated through depletion of ER Ca<sup>2+</sup> stores by inositol 1,4,5-trisphosphate (InsP<sub>3</sub>) and store-independent activation that is mediated by cell dialysis during whole-cell perfusion. Both modes are regulated by calmodulin (CaM). The store-operated mode is transient in intact cells, possibly reflecting recruitment of CaM, whereas loss of CaM in perfused cells accounts for the persistence of the store-independent mode. The inhibition by CaM can be reversed by 2-aminoethoxydiphenyl borate (2-APB), resulting in rapid, store-independent activation of CRAC channels. The aminoglycoside antibiotic G418 is a highly specific and potent inhibitor of STIM2-dependent CRAC channel activation. The results reveal a novel bimodal control of CRAC channels by STIM2, the store dependence and CaM regulation, which indicates that the STIM2/CRACM1 complex may be under the control of both luminal and cytoplasmic Ca<sup>2+</sup> levels.—Parvez, S., Beck, A., Peinelt, C., Soboloff, J., Lis, A., Monteilh-Zoller, M., Gill, D. L., Fleig, A., Penner, R. STIM2 protein mediates distinct store-dependent and store-independent modes of CRAC channel activation. *FASEB J.* 22, 000–000 (2008)

*Key Words:* STIM1 • calmodulin • store-operated calcium entry

CHANGES IN INTRACELLULAR free calcium concentration ([Ca<sup>2+</sup>]<sub>i</sub>) represent one of the most widespread and important signaling events, regulating a plethora of cellular responses. Many cell types employ store-operated Ca<sup>2+</sup> entry (SOCE) as their principal pathway for Ca<sup>2+</sup> influx (1–3). This mechanism is engaged after

Ca<sup>2+</sup> release from stores, where the depleted stores lead to activation of Ca<sup>2+</sup> release-activated Ca<sup>2+</sup> (CRAC) channels (4–6). Recent work (7–11) has identified STIM1 and CRACM1 (or Orai1) as essential components for functional SOCE. When overexpressed jointly, but not individually, STIM1 and CRACM1 reconstitute large CRAC currents (11–14). In mammals, there exist several homologs of these proteins: STIM1 and STIM2 in the endoplasmic reticulum (ER) and CRACM1, CRACM2, and CRACM3 in the plasma membrane. On Ca<sup>2+</sup> depletion of stores, STIM1 translocates into junctional structures close to the plasma membrane (8, 15–17), where it may bind to and activate CRACM1 (18, 19). Mutational analysis revealed that several key amino acids in CRACM1 determine the selectivity of CRAC currents, demonstrating that CRACM1 forms the ion-selective pore of the CRAC channel (18–20).

All three CRACM homologs represent functional store-operated channels with differential properties (12, 21, 22). The role of STIM2 in SOCE appears to be complex and remains incompletely understood. When overexpressed alone, STIM2 inhibits SOCE (16), yet coexpressed with CRACM1, STIM2 causes constitutive rather than store-dependent Ca<sup>2+</sup> entry that is strongly enhanced by 2-aminoethoxydiphenyl borate (2-APB; ref. 14). When expressed in HEK293 cells, this protein resides exclusively in the ER, but unlike STIM1, it does not redistribute into junctions after store depletion, unless STIM1 is also overexpressed (16). To gain insight into the functional properties of STIM2, we performed a careful analysis of how it regulates CRAC channels.

<sup>1</sup> These authors contributed equally to this work.

<sup>2</sup> Correspondence: Center for Biomedical Research, The Queen's Medical Center, 1301 Punchbowl St., UHT 8, Honolulu, HI 96813, USA. E-mail: rpenner@hawaii.edu  
doi: 10.1096/fj.07-9449com

## MATERIALS AND METHODS

### Subcloning and overexpression of CRACM and STIM

Full-length human CRACM1, CRACM2, and CRACM3 were subcloned as described previously (18, 22). For electrophysiological analysis, CRACM proteins were overexpressed in HEK293 cells stably expressing STIM1 and STIM2 (16) using lipofectamine 2000 (Invitrogen, Carlsbad, CA, USA). Experiments were performed 24–48 h post-transfection. For the experiments with HEK293 cells stably expressing STIM2, cells were grown for several days or weeks in the absence or presence of G418 (500  $\mu\text{g}/\text{ml}$ ). Green cells were analyzed for the effects of CRACM overexpression.

### Electrophysiology

Patch-clamp experiments were performed in the tight-seal whole-cell configuration at 21–25°C. High-resolution current recordings were acquired using the EPC-9 (HEKA). Voltage ramps of 50 ms duration spanning a range of  $-100$  to  $+100$  mV were delivered from a holding potential of 0 mV at a rate of 0.5 Hz over a period of 100–700 s. All voltages were corrected for a liquid junction potential of 10 mV (3 mV with  $\text{Cl}^-$  as main internal anion). Currents were filtered at 2.9 kHz and digitized at 100  $\mu\text{s}$  intervals. Capacitive currents were determined and corrected before each voltage ramp. Extracting the current amplitude at  $-80$  mV from individual ramp current records assessed the low-resolution temporal development of currents. Where applicable, statistical errors of averaged data are mean  $\pm$  SE with  $n$  determinations. Standard external solutions were as follows (in mM): 120 NaCl, 10 CsCl, 2.8 KCl, 2  $\text{MgCl}_2$ , 10  $\text{CaCl}_2$ , 10 TEA-Cl, 10 HEPES, and 10 glucose, pH 7.2 with NaOH, 300 mosM. In some experiments, 2, 5, or 50  $\mu\text{M}$  2-APB or 10  $\mu\text{M}$  G418 was added to the standard external solution and applied through wide-tipped puffer pipettes. Standard internal solutions were as follows (in mM): 120 Cs-glutamate, 8 NaCl, 20 Cs-BAPTA, 3  $\text{MgCl}_2$ , 10 HEPES, and 0.02 inositol 1,4,5-trisphosphate ( $\text{InsP}_3$ ), pH 7.2 with CsOH, 300 mosM. As indicated in the figure legends, for some experiments  $[\text{Ca}^{2+}]_i$  was buffered to 150 or 100 nM by 20 mM Cs-BAPTA and 8 mM  $\text{CaCl}_2$  or 10 mM Cs-EGTA and 3.6 mM  $\text{CaCl}_2$ , respectively. For passive-depletion experiments, the internal solution was supplemented with Cs-BAPTA in the absence of  $\text{InsP}_3$  and  $\text{Ca}^{2+}$ . In some experiments, Cs-glutamate and Cs-BAPTA were equimolarly replaced by KCl and K-BAPTA. In others, G418, Na-ATP and Na-GTP, or calmodulin (CaM) were added to intracellular solutions as specified in the figure legends. All chemicals were purchased from Sigma-Aldrich (St. Louis, MO, USA).

### Fluorescence Measurements

Cells grown on coverslips were placed in external solution containing (in mM): 107 NaCl, 7.2 KCl, 1  $\text{CaCl}_2$ , 1.2  $\text{MgCl}_2$ , 11.5 glucose, and 10 HEPES, pH 7.2 with NaOH, and loaded with fura-2 acetoxymethyl ester (2  $\mu\text{M}$ ) for 30 min at 20°C. Cells were washed, and dye was allowed to de-esterify for a minimum of 30 min at 20°C. Approximately 95% of the dye was confined to the cytoplasm as determined by the signal remaining after saponin permeabilization. Cells on coverslips were placed in external solution in the absence or presence of 1 mM  $\text{CaCl}_2$ .  $\text{Ca}^{2+}$  measurements were made using an InCyt dual-wavelength fluorescence imaging system (Intracellular Imaging Inc., Cincinnati, OH, USA). Fluorescence emission at 505 nm was monitored with excitation at 340 and 380 nm; intracellular  $\text{Ca}^{2+}$  measurements are shown as 340/380 nm ratios obtained from groups (35–45) of single cells. The

details of these  $\text{Ca}^{2+}$  measurements were described previously (23). All measurements shown represent minimum of three independent experiments.

## RESULTS

Initial experiments, in which we compared CRAC currents in HEK293 cells stably overexpressing STIM1 or STIM2, confirmed that both proteins slightly modify endogenous  $I_{\text{CRAC}}$ . In response to  $\text{Ca}^{2+}$  store depletion by  $\text{InsP}_3$ , STIM2-expressing cells exhibited reduced  $I_{\text{CRAC}}$  ( $\sim 0.2$  pA/pF) and STIM1-expressing cells had slightly increased  $I_{\text{CRAC}}$  ( $\sim 0.7$  pA/pF) compared to wild-type cells ( $\sim 0.5$  pA/pF; see Fig. 1A; ref. 13). To investigate the functional interaction of STIM proteins with CRACM1, HEK293 cells stably overexpressing STIM1 or STIM2 were transiently transfected with CRACM1 and  $I_{\text{CRAC}}$  was measured in response to  $\text{InsP}_3$ . Consistent with our previous observations (13, 14), STIM1 cells generated large CRAC currents, whereas STIM2 cells did not (Fig. 1B). Although we did not observe readily discernable constitutive CRAC channel activity corresponding to the previously described  $\text{Ca}^{2+}$  entry (14), a small basal CRAC current of  $<1$  pA/pF at break-in could have gone unnoticed. However, a small CRAC current developed very slowly, on average amounting to approximately  $-1$  pA/pF at  $-80$  mV. Under identical experimental conditions, despite the lack of  $\text{InsP}_3$ -induced CRACM1 currents, external application of 2-APB (2  $\mu\text{M}$ ) induced large CRACM1 currents with the typical inwardly rectifying current-voltage ( $I$ - $V$ ) relationships (Fig. 1B, C). 2-APB is a compound that has facilitatory effects on CRAC currents at low doses ( $\leq 5$   $\mu\text{M}$ ) but inhibits them at high doses ( $\geq 10$   $\mu\text{M}$ ; refs. 23–26). In cells expressing STIM2 and CRACM1, 2-APB applied at 50  $\mu\text{M}$  caused a rapid, large, and transient activation of CRAC current (Fig. 1D). In these experiments, we omitted  $\text{InsP}_3$  from the patch pipette and also buffered  $[\text{Ca}^{2+}]_i$  to 150 nM to keep stores repleted, so the 2-APB effect observed here did not require store depletion.

To better resolve the kinetics of this response, we performed high-resolution recordings of the 2-APB effect at a fixed membrane potential of  $-80$  mV. Figure 1E shows that the large 2-APB-induced current peaked within  $\sim 8$  s and disappeared to almost zero within a further 10 s. This 2-APB-induced effect was specific to cells overexpressing STIM2 and CRACM1, since it was not observed in HEK293 cells that overexpressed either STIM2 or CRACM1 alone or a combination of STIM1 and CRACM1 (Fig. 1D). The 2-APB-induced activation seems to be too rapid to be mediated by store-dependent translocation of STIM2 to couple to CRACM1. We therefore surmise that a significant portion of CRACM1 channels must somehow be in a readily activated state, possibly precoupled in a complex with STIM2. Immunofluorescence analysis reveals that STIM2 is distributed in ER structures throughout the cell but is also found close to the plasma membrane, where it partially

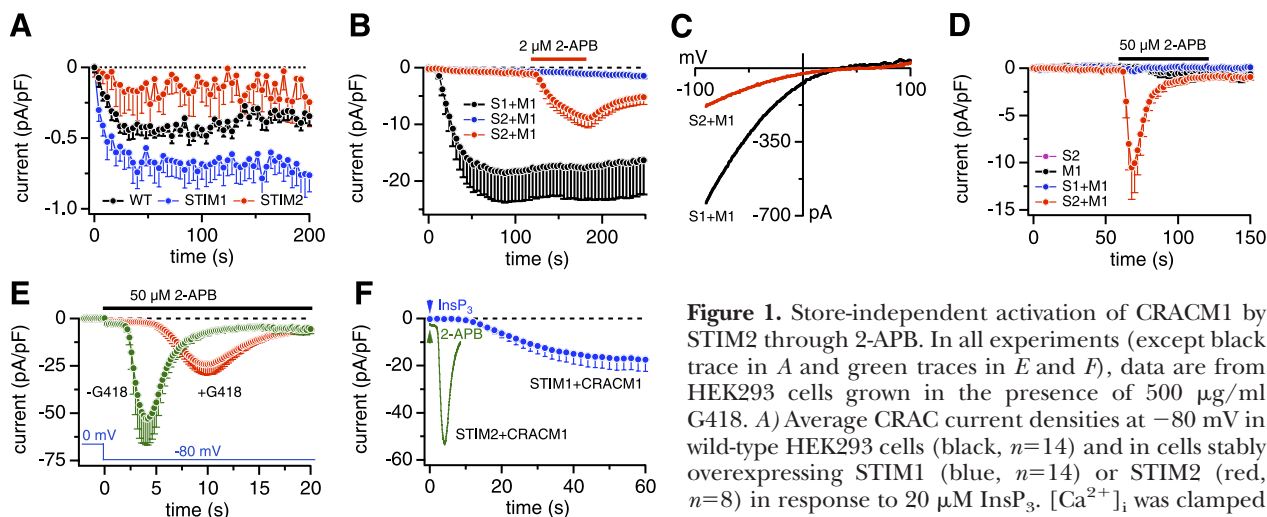


**Figure 1.** Store-independent activation of CRACM1 by STIM2 through 2-APB. In all experiments (except black trace in *A* and green traces in *E* and *F*), data are from HEK293 cells grown in the presence of 500  $\mu\text{g}/\text{ml}$  G418. *A*) Average CRAC current densities at  $-80$  mV in wild-type HEK293 cells (black,  $n=14$ ) and in cells stably overexpressing STIM1 (blue,  $n=14$ ) or STIM2 (red,  $n=8$ ) in response to  $20$   $\mu\text{M}$   $\text{InsP}_3$ .  $[\text{Ca}^{2+}]_i$  was clamped to near zero with  $20$  mM BAPTA. *B*) Average CRAC current densities induced by  $20$   $\mu\text{M}$   $\text{InsP}_3$  +  $20$  mM BAPTA in STIM1+CRACM1 cells (black,  $n=15$ ), STIM2+CRACM1 cells (blue,  $n=10$ ), and STIM2+CRACM1 cells stimulated by  $2$   $\mu\text{M}$  2-APB (red,  $n=9$ ). *C*) Representative current-voltage (I/V) relationships of CRAC currents in STIM1+CRACM1-expressing cells or  $2$   $\mu\text{M}$  2-APB-induced currents in STIM2+CRACM1-expressing cells shown in *B*. *D*) Average CRAC current densities in HEK293 cells expressing STIM2 alone (purple,  $n=5$ ; trace is flat around  $0$  pA/pF and masked by blue trace), CRACM1 alone (black,  $n=3$ , trace is flat around  $0$  pA/pF and masked by blue trace), STIM1+CRACM1 (blue,  $n=8$ ), and STIM2+CRACM1 (red,  $n=9$ ). In all cells,  $[\text{Ca}^{2+}]_i$  was buffered to  $150$  nM using  $20$  mM BAPTA and  $8$  mM  $\text{CaCl}_2$ . *E*) High-resolution average CRAC currents at  $-80$  mV in STIM2+CRACM1 cells grown in the presence (red,  $n=7$ ) or absence (green,  $n=5$ ) of G418 induced by  $50$   $\mu\text{M}$  2-APB as in *D*. *F*) Comparison of activation kinetics of  $\text{InsP}_3$ - and 2-APB-induced gating of CRAC channels. Data sets are taken from *B* and *E* and plotted on same time scale to illustrate speed of STIM2-dependent and 2-APB-induced activation relative to STIM1-dependent and store-operated activation of CRACM1.

current densities induced by  $20$   $\mu\text{M}$   $\text{InsP}_3$  +  $20$  mM BAPTA in STIM1+CRACM1 cells (black,  $n=15$ ), STIM2+CRACM1 cells (blue,  $n=10$ ), and STIM2+CRACM1 cells stimulated by  $2$   $\mu\text{M}$  2-APB (red,  $n=9$ ). *C*) Representative current-voltage (I/V) relationships of CRAC currents in STIM1+CRACM1-expressing cells or  $2$   $\mu\text{M}$  2-APB-induced currents in STIM2+CRACM1-expressing cells shown in *B*. *D*) Average CRAC current densities in HEK293 cells expressing STIM2 alone (purple,  $n=5$ ; trace is flat around  $0$  pA/pF and masked by blue trace), CRACM1 alone (black,  $n=3$ , trace is flat around  $0$  pA/pF and masked by blue trace), STIM1+CRACM1 (blue,  $n=8$ ), and STIM2+CRACM1 (red,  $n=9$ ). In all cells,  $[\text{Ca}^{2+}]_i$  was buffered to  $150$  nM using  $20$  mM BAPTA and  $8$  mM  $\text{CaCl}_2$ . *E*) High-resolution average CRAC currents at  $-80$  mV in STIM2+CRACM1 cells grown in the presence (red,  $n=7$ ) or absence (green,  $n=5$ ) of G418 induced by  $50$   $\mu\text{M}$  2-APB as in *D*. *F*) Comparison of activation kinetics of  $\text{InsP}_3$ - and 2-APB-induced gating of CRAC channels. Data sets are taken from *B* and *E* and plotted on same time scale to illustrate speed of STIM2-dependent and 2-APB-induced activation relative to STIM1-dependent and store-operated activation of CRACM1.

overlaps with CRACM1 localization (Fig. 2B). Store depletion had no effect on this distribution of STIM2. This is in contrast to STIM1, which redistributes into CRACM1-associated junctions after store depletion (Fig. 2A). Interestingly, coimmunoprecipitation experiments revealed that not only STIM1 but also STIM2 can physically interact with CRACM1 (Fig. 2C), which indicates that both STIM proteins interact with CRACM1. If STIM2 and CRACM1 exist coupled without store depletion and can generate large CRAC currents in response to 2-APB, what prevents the CRACM1 channel from being open? As described here, it appears that an endogenous inhibitor prevents activation of the channel and that 2-APB reverses the action of this inhibitor.

Interestingly, the distinct effect of STIM2 could be selectively modified by the aminoglycoside antibiotic G418. G418 is routinely present at  $500$   $\mu\text{g}/\text{ml}$  ( $720$   $\mu\text{M}$ ) in the growth medium to maintain selection pressure on cells stably transfected with STIM1 or STIM2. HEK293 cells grown for several days in the absence of G418 exhibited enhanced responses to 2-APB and strikingly different responses to store depletion, yet there was no significant decrease in protein levels (Fig. 2D). As shown in Fig. 1E, these cells responded with even faster kinetics and with larger current amplitudes to  $50$   $\mu\text{M}$  2-APB. To appreciate the speed of this response, Fig. 1F superimposes the fastest possible store-operated activation of CRACM1 through STIM1 using  $\text{InsP}_3$  as a stimulus and the 2-APB-mediated activation of CRACM1 through STIM2, demonstrating that full activation of CRACM1 in STIM2-expressing

cells is complete before the activation of STIM1-mediated CRAC currents even begins. These results suggest that the aminoglycoside inhibits store-operated gating of CRAC channels through STIM2 and that 2-APB can overcome this inhibition. This effect of G418 was specific to STIM2, since STIM1-expressing cells, which were also routinely grown in G418, produced large CRACM1-mediated currents (see Fig. 1B) with similar properties as those produced by transient coexpression of STIM1 and CRACM1 in HEK293 cells that remained unexposed to G418 (13, 18).

The removal of G418 provided an important condition under which to analyze STIM2 activation in response to store depletion. Thus, in cells not exposed to G418,  $\text{InsP}_3$  perfusion now generated amplified CRAC currents (Fig. 3A). These CRAC currents were characterized by a biphasic activation pattern consisting of an initial fast activation phase followed by a slower phase that set in after  $\sim 100$  s and rarely reached steady state within  $300$  s. The relative proportion of the two phases was somewhat variable across experimental days and may reflect the different coupling mechanisms of STIM2 populations (see below). Typical current amplitudes at  $-80$  mV obtained  $300$  s into the experiment were approximately  $-15$  pA/pF and had the signature I/V curves typical of CRAC currents (Fig. 3B).

Since STIM1 can activate all three CRACM homologs (22), we examined whether STIM2 could also couple to CRACM2 and CRACM3. Figure 3A demonstrates that this is indeed the case. Coexpression of STIM2 with any of the three homologs produced biphasic currents, although the secondary phase of activation was less

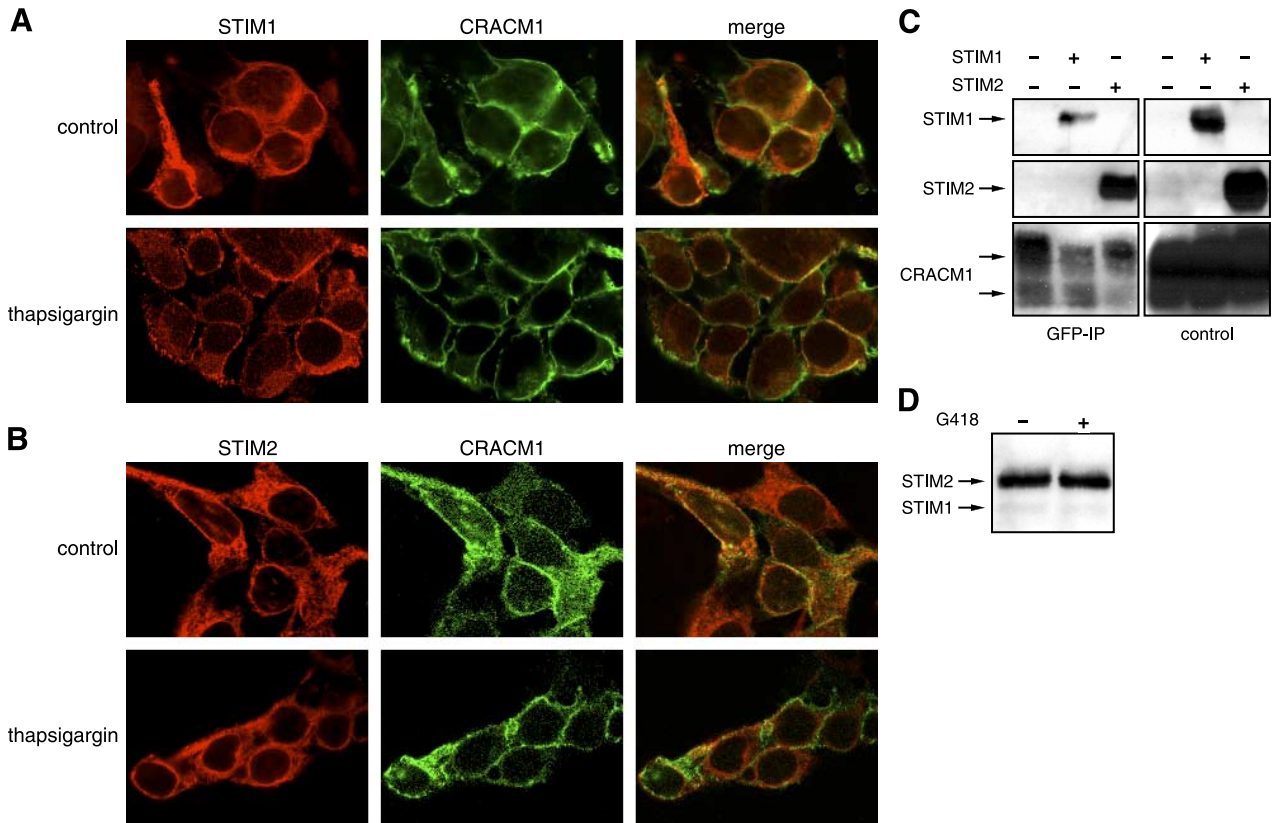


**Figure 2.** Immunolocalization of STIM and CRACM proteins. Images were obtained by confocal microscopy, while colocalization (yellow) was demonstrated by merging the images using ImageJ software (NIH). *A*) Cells stably expressing CFP-CRACM1 (green) were transfected with STIM1 (red), treated with 2  $\mu$ M thapsigargin for 10 min, and then fixed, permeabilized, and blocked. Cells were sequentially double-stained with sheep STIM1-specific and rabbit anti-GFP antibodies (Invitrogen), followed by corresponding 2<sup>o</sup> antibodies. *B*) Cells stably expressing STIM2 (red) were transfected with CFP-CRACM1 (green), treated with 2  $\mu$ M thapsigargin for 10 min, and then fixed, permeabilized, and blocked. Cells were sequentially double-stained with sheep STIM2-specific and rabbit anti-GFP antibodies (Invitrogen), followed by corresponding 2<sup>o</sup> antibodies. *C*) Binding of STIM proteins to CRACM1 was assessed after transient transfection of STIM1 or STIM2 into HEK293 cells stably expressing CRACM1. Approximate molecular masses of proteins were 85 kDa for STIM1, 105 kDa for STIM2, and 55 kDa for CFP-CRACM1, the glycosylated form of which is  $\sim$ 70 kDa. After transfection, cells were lysed and the proteins were quantified. For immunoprecipitations, 200  $\mu$ g of protein/sample were incubated with protein G beads coated with rabbit anti-GFP antibodies (Invitrogen) for 2 h followed by separation with SDS-PAGE and transfer to PVDF membranes. Protein expression was confirmed by loading 5  $\mu$ g of untransfected lysate. STIM proteins were detected by Western blot using an antibody cross-reacting with both STIM1 and STIM2 (BD Biosciences, San Jose, CA, USA), while pulldown and expression of CFP-CRACM1 was demonstrated by stripping and reprobing a goat-anti-GFP antibody (Abcam). *D*) STIM2-expressing cells were incubated for 3 wk in the presence or absence of G418. Cells were lysed and the proteins were quantified. Proteins (5  $\mu$ g/sample) were separated by SDS-PAGE and transferred to PVDF membranes. Levels of STIM expression were demonstrated by Western blot with an antibody cross-reacting to both STIM1 and STIM2 (BD Biosciences).

pronounced in CRACM2- and CRACM3-expressing cells. The I/V relationships of these currents were very similar and exhibited typical CRAC inward rectification (Fig. 3B), suggesting that both STIM homologs can couple to any of the CRACM homologs to activate store-operated currents.

It is important to ascertain that the InsP<sub>3</sub>-induced currents observed in Fig. 3A developed as a consequence of store depletion. Therefore, we performed additional experiments in which store depletion was induced independently of InsP<sub>3</sub>. We first examined whether CRAC currents were activated when preventing store refilling with 20 mM BAPTA in the pipette. This also produced large CRAC-like currents but with a significant delay (Fig. 3C, blue trace), which would be consistent with the time needed to passively deplete

stores through leak pathways. We then performed the same experiments but used the Ca<sup>2+</sup> ionophore ionomycin to rapidly release Ca<sup>2+</sup> from intracellular stores (Fig. 3C, black trace). With this protocol, we observed biphasic activation of CRACM1 currents that were similar in both amplitude and kinetics to those activated by InsP<sub>3</sub>. If both phases of CRAC current were store-dependent, we should have been able to suppress current activation entirely by perfusing cells with an InsP<sub>3</sub>-free solution and buffering [Ca<sup>2+</sup>]<sub>i</sub> to 150 nM to avoid store depletion. As can be seen in Fig. 3D (green trace), these conditions indeed prevent store-dependent activation of CRAC currents in STIM1- and CRACM1-expressing cells. Surprisingly, however, the same experimental conditions still generated the slow secondary phase in STIM2- and CRACM1-expressing

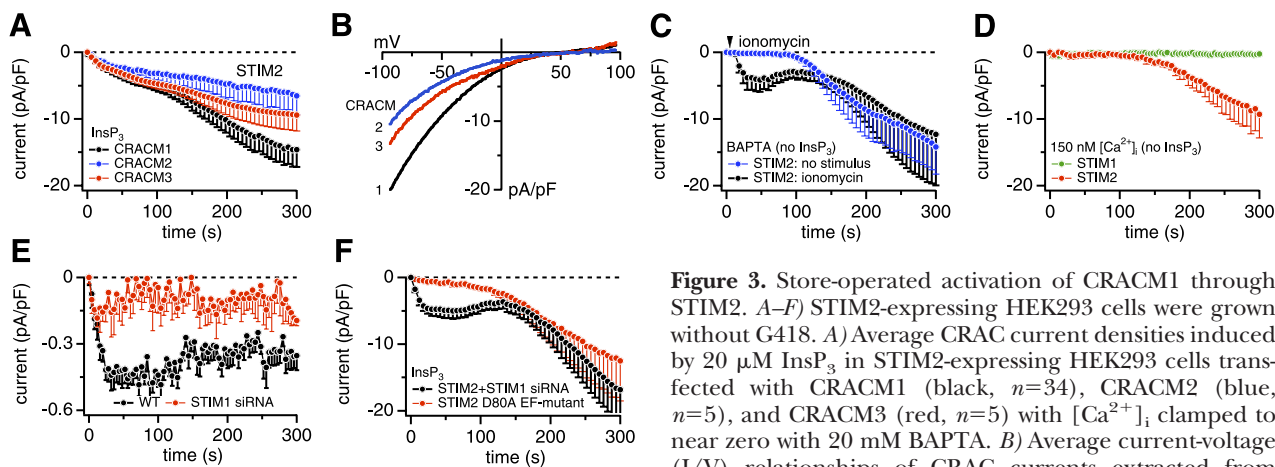


**Figure 3.** Store-operated activation of CRACM1 through STIM2. *A–F*) STIM2-expressing HEK293 cells were grown without G418. *A*) Average CRAC current densities induced by 20  $\mu\text{M}$   $\text{InsP}_3$  in STIM2-expressing HEK293 cells transfected with CRACM1 (black,  $n=34$ ), CRACM2 (blue,  $n=5$ ), and CRACM3 (red,  $n=5$ ) with  $[\text{Ca}^{2+}]_i$  clamped to near zero with 20 mM BAPTA. *B*) Average current-voltage (I/V) relationships of CRAC currents extracted from

representative STIM2+CRACM1, 2, and 3 cells shown in *A* at 300 s into experiment. Data represent leak-subtracted currents evoked by 50 ms voltage ramps from  $-100$  to  $+100$  mV, normalized to cell capacitance (pA/pF). *C*) Average CRAC current densities in STIM2-expressing HEK293 cells transfected with CRACM1, where  $[\text{Ca}^{2+}]_i$  was clamped to near zero with 20 mM BAPTA to induce passive store depletion (blue,  $n=7$ ). In other cells (black,  $n=6$ ), active store depletion was induced by brief (2 s) application of 2  $\mu\text{M}$  ionomycin (indicated by the arrow). *D*) Average CRAC current densities in STIM1- (green,  $n=6$ ) or STIM2-expressing HEK293 cells (red,  $n=7$ ) transfected with CRACM1, where store depletion was prevented by omission of  $\text{InsP}_3$  and buffering  $[\text{Ca}^{2+}]_i$  to 150 nM with 20 mM BAPTA + 8 mM  $\text{CaCl}_2$ . *E*) Average CRAC current densities at  $-80$  mV in wt HEK293 cells (black,  $n=14$ ) or cells treated with STIM1-specific siRNA (red,  $n=6$ ) in response to 20  $\mu\text{M}$   $\text{InsP}_3$ .  $[\text{Ca}^{2+}]_i$  was clamped to near zero with 20 mM BAPTA. Data demonstrate that STIM1 siRNA treatment was effective and suppressed native CRAC currents. *F*) Average CRAC current densities in STIM2+CRACM1 cells that were cotransfected with siRNA against STIM1 (black,  $n=5$ ) in parallel and exactly as in *E*. Average CRAC current densities in CRACM1-expressing cells that were cotransfected with the D80A EF-hand mutant of STIM2 (red,  $n=5$ ). In both experimental sets, store depletion was induced by 20  $\mu\text{M}$   $\text{InsP}_3$  and  $[\text{Ca}^{2+}]_i$  buffered to near zero by 20 mM BAPTA.

cells (Fig. 3*D*, red trace). These results indicate that the first phase of the CRAC current is indeed caused by store depletion, but the second phase develops regardless of the filling state of intracellular stores and is store independent. As we reveal below, this secondary, store-independent phase of current activation appears to be caused by the diffusional escape of  $\text{Ca}^{2+}$ -CaM into the patch pipette during perfusion of cells in patch-clamp recordings.

Although the above experiments suggest that store depletion *via*  $\text{InsP}_3$  or ionomycin results in activation of CRAC channels, the store dependence of STIM2 could have resulted from its comigration with STIM1 into junctions. We therefore examined whether STIM2 can serve as a  $\text{Ca}^{2+}$  sensor and activate CRAC channels in a store-dependent manner when STIM1 expression was suppressed by small interfering RNA (siRNA). We confirmed the efficacy of siRNA treatment in wild-type (wt) HEK293 cells, where endogenous CRAC currents were almost completely suppressed after siRNA treatment (Fig. 3*E*). However, in parallel experiments performed in STIM2- and CRACM1-expressing cells, STIM1 knockdown did not significantly affect the biphasic CRAC currents (Fig. 3*F*), suggesting that STIM2 has the intrinsic ability to respond to store depletion. We surmised that the  $\text{Ca}^{2+}$ -sensing function of STIM2 might be mediated by an EF-hand motif located in the N terminus of the protein facing the lumen of the ER, since such a motif is also found in STIM1 and has been shown to serve this function (8, 17, 27). To test this idea, we introduced a point mutation into the EF-hand motif of the STIM2 protein (D80A) that would be

predicted to disrupt  $\text{Ca}^{2+}$  binding. The equivalent mutation in STIM1 (D76A) has been shown to abolish its  $\text{Ca}^{2+}$ -sensing function and results in constitutive activation of SOCE (8, 17, 27). As illustrated in Fig. 3*F*, the D80A mutant of STIM2 failed to support the rapid, store-operated activation phase of CRAC channels, whereas the delayed, store-independent activation phase remained unaffected. Together, these results suggest that STIM2 can mediate both store-operated and store-independent activation of CRAC channels independent of STIM1 and that the  $\text{Ca}^{2+}$ -sensing function of STIM2 resides within its luminal EF-hand motif.

Since the cells grown in the absence of G418 responded to  $\text{InsP}_3$ -induced store depletion, we were able to assess the inhibitory effect of this antibiotic on STIM2-mediated activation of CRACM1 by perfusing cells with defined concentrations of G418. **Figure 4A** illustrates the dose-dependent inhibition of both phases of the  $\text{InsP}_3$ -induced CRACM1 currents by increasing concentrations of G418, resulting in a half-maximal inhibitory concentration of  $\sim 0.6$   $\mu\text{M}$  (Fig. 4*B*). Under identical experimental conditions, where 10  $\mu\text{M}$  G418 was perfused intracellularly, it did not modify  $\text{InsP}_3$ -induced CRAC currents in STIM1- and CRACM1-coexpressing cells (Fig. 4*C*). Although the most potent effect of G418 appears to be mediated from the intracellular space and specifically affects STIM2-expressing cells, we also observed some small inhibition of the aminoglycoside when it was applied at 10  $\mu\text{M}$  from the extracellular side. This effect, however, did not seem to be specific for STIM2, since it was similar in both STIM1- and STIM2-expressing cells (Fig.

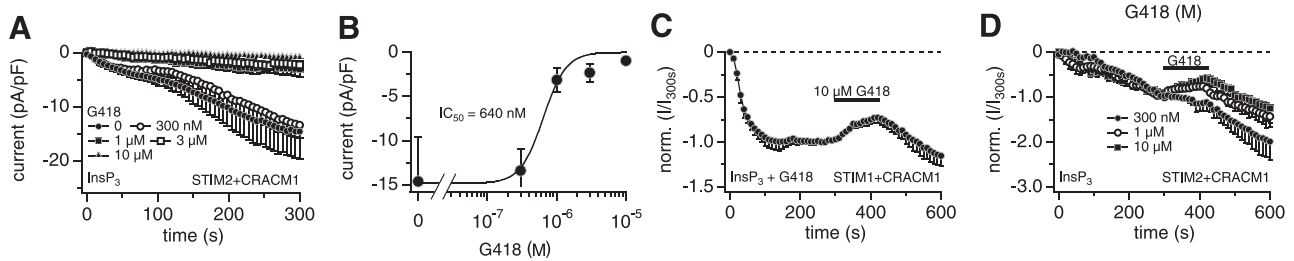


**Figure 4.** Effects of G418 on STIM1- and STIM2-mediated activation of CRACM1. *A*) Average CRAC current densities in STIM2+CRACM1 cells in the absence of G418 (closed circles,  $n=34$ ) or presence of 300 nM (open circles,  $n=9$ ), 1  $\mu\text{M}$  (closed squares,  $n=11$ ), 3  $\mu\text{M}$  (open squares,  $n=8$ ), or 10  $\mu\text{M}$  (closed triangles,  $n=8$ ) of G418 in the pipette. *B*) Dose-response relationship of average CRAC current densities as a function of G418 concentration extracted at 300 s from the recordings shown in *E*. Data were fitted with a dose-response curve, yielding an  $\text{IC}_{50}$  value of 640 nM and a Hill coefficient of 2.6. *C*) Average CRAC currents in STIM1+CRACM1 cells ( $n=7$ ) grown in the presence of G418. Pipette solutions contained  $\text{InsP}_3$  (20  $\mu\text{M}$ ) and 10  $\mu\text{M}$  G418, demonstrating that these cells are largely insensitive to intracellular G418. Extracellular application of 10  $\mu\text{M}$  G418 caused a small and reversible reduction in CRAC current. *D*) Effects of extracellularly applied G418 on STIM2+CRACM1. Average CRAC currents in STIM2+CRACM1 cells grown without G418. Pipette solutions contained  $\text{InsP}_3$  (20  $\mu\text{M}$ ) to activate biphasic CRAC currents. Bar indicates extracellular application of various concentrations of G418. These caused a small and reversible reduction in CRAC current: 300 nM (filled circles,  $n=3$ ), 1  $\mu\text{M}$  (open circles,  $n=4$ ), and 10  $\mu\text{M}$  (filled squares,  $n=5$ ).

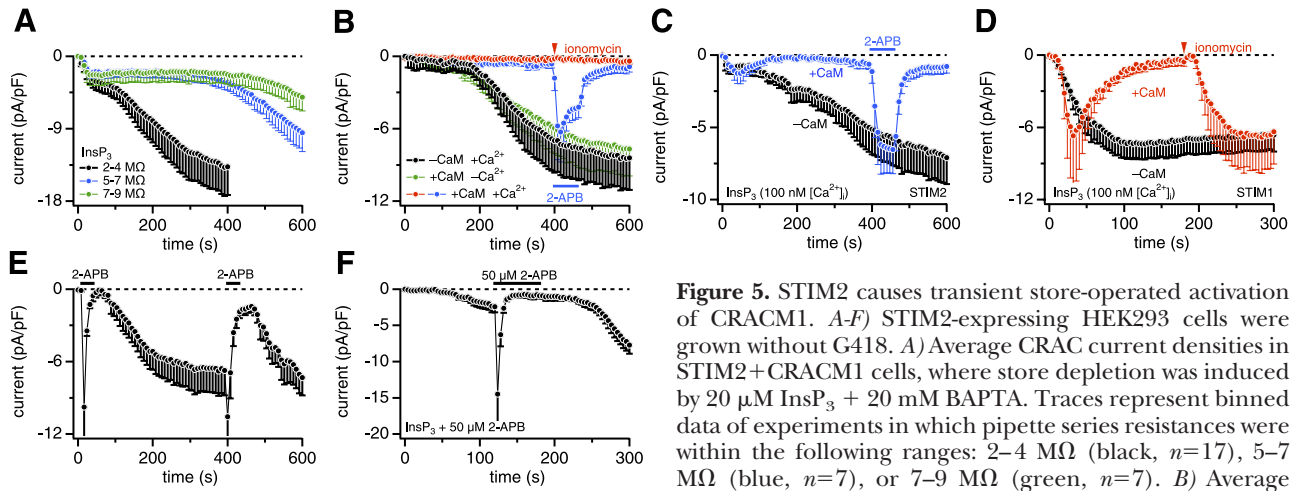
4C, D), suggesting that it might be a pharmacological effect on CRACM1. The specific and potent inhibition of STIM2-mediated CRAC currents caused by intracellular G418 (and possibly other aminoglycoside antibiotics) thus may provide a powerful pharmacological tool to assess STIM2 function in native cell systems.

Figure 3 shows CRAC currents that developed during active store depletion by  $\text{InsP}_3$ , which caused the typical biphasic activation of CRACM1 currents, with the first phase being store-operated, whereas the second phase developed independent of the filling state of stores. Hence, the secondary phase is either activated by some ingredient of our pipette filling solution or it is caused by the loss of some cytosolic factor that constitutively suppresses CRAC channels. We tested for these possibilities by exchanging the major ingredients of the standard pipette filling solution. However, the substitution of the primary intracellular salt Cs-glutamate with KCl ( $n=5$ , data not shown) and the replacement of BAPTA with EGTA (see Fig. 5B) were both ineffective in suppressing the secondary current component. Thus, we conclude that the secondary CRAC current phase is likely to result from the washout of a cellular factor. To substantiate this idea, we performed experiments in which we varied pipette tip diameters and analyzed biphasic currents. Smaller pipette tips (with higher series resistance) would reduce the rate of diffusional escape of the cytosolic inhibitor, and Fig. 5A demonstrates that this indeed delayed the development of the secondary phase. The cytosolic factor does not appear to be either of the two major cytosolic nucleotides, since adding physiological concentrations of ATP (3 mM) and GTP (0.3 mM) failed to suppress the secondary phase ( $n=5$ ; data not shown).

We next considered CaM as a possible factor, since CaM can regulate numerous ion channels (28), including CRAC channels (29, 30). We performed experiments in which  $[\text{Ca}^{2+}]_i$  was buffered to near resting levels of  $\sim 100$  nM using EGTA as chelator and CaM was either omitted or included in the pipette filling solu-

tion. In the absence of CaM, with  $[\text{Ca}^{2+}]_i$  buffered to resting levels, the CRAC current activated after a delay (Fig. 5B, black trace), similar to the experiments described in Fig. 3D (red trace), where BAPTA was used as chelator. However, additional inclusion of CaM (100  $\mu\text{M}$ ) essentially prevented the store-independent activation of CRAC currents (Fig. 5B, red and blue traces), suggesting that CaM may indeed represent the sought cytosolic inhibitor. Subsequent exposure of cells to ionomycin (Fig. 5B, red trace) to deplete stores was ineffective in activating CRAC currents, but channels remained activable by 5  $\mu\text{M}$  2-APB (Fig. 5B, blue trace). The inhibitory effect of CaM required some  $[\text{Ca}^{2+}]_i$ , since the same concentration of CaM failed to suppress CRAC current activation when  $[\text{Ca}^{2+}]_i$  was clamped to near zero with 10 mM EGTA and no added  $\text{Ca}^{2+}$  (Fig. 5B, green trace). Thus, STIM2-mediated CRAC currents are inhibited by  $\text{Ca}^{2+}$ -bound CaM but not by resting  $[\text{Ca}^{2+}]_i$  alone or  $\text{Ca}^{2+}$ -free apo-CaM. We further confirmed that CaM can inhibit store-operated CRAC channel activation by perfusing cells with both  $\text{InsP}_3$  and CaM and  $[\text{Ca}^{2+}]_i$  buffered to 100 nM (Fig. 5C, blue trace). This resulted in a transient CRAC current, presumably due to fast  $\text{InsP}_3$ -mediated store depletion and STIM2-mediated activation of CRACM1, which was then curtailed by inhibition through CaM as it accumulated intracellularly. CaM also prevented the secondary, store-independent CRAC current phase, normally seen in the absence of CaM (Fig. 5C, black trace). Nevertheless, the CRAC channels remained available for activation by 5  $\mu\text{M}$  2-APB and were suppressed again by CaM on washout of 2-APB.

The inhibitory effect of CaM could occur at various points in the signal transduction process of SOCE, including  $\text{InsP}_3$  receptors, STIM sensors, and/or CRAC channels. We examined this issue by performing experiments in STIM1- and CRACM1-expressing cells under identical experimental conditions as those for STIM2 shown in Fig. 5C. With  $[\text{Ca}^{2+}]_i$  buffered to near resting levels of  $\sim 100$  nM and CaM absent from the pipette



**Figure 5.** STIM2 causes transient store-operated activation of CRACM1. *A-F*) STIM2-expressing HEK293 cells were grown without G418. *A*) Average CRAC current densities in STIM2+CRACM1 cells, where store depletion was induced by 20  $\mu\text{M}$   $\text{InsP}_3$  + 20 mM BAPTA. Traces represent binned data of experiments in which pipette series resistances were within the following ranges: 2–4 M $\Omega$  (black,  $n=17$ ), 5–7 M $\Omega$  (blue,  $n=7$ ), or 7–9 M $\Omega$  (green,  $n=7$ ). *B*) Average CRAC current densities in STIM2+CRACM1 cells. CRAC currents developed normally both in the absence of added CaM with  $[\text{Ca}^{2+}]_i$  buffered to 100 nM with 10 mM EGTA + 3.6 mM  $\text{CaCl}_2$  (black,  $n=5$ ) or in its presence (100  $\mu\text{M}$ ) with  $[\text{Ca}^{2+}]_i$  buffered to 0 with 10 mM EGTA and no added  $\text{Ca}^{2+}$  (green,  $n=9$ ). However, CRAC currents were suppressed by the combined presence of 100  $\mu\text{M}$  CaM and 100 nM  $[\text{Ca}^{2+}]_i$  (blue,  $n=7$ ; red,  $n=4$ ). Application of 2  $\mu\text{M}$  ionomycin for 3 s (red) or 5  $\mu\text{M}$  2-APB for 60 s (blue) is indicated in graph. *C*) Average CRAC currents in STIM2+CRACM1 cells induced by 20  $\mu\text{M}$   $\text{InsP}_3$  with  $[\text{Ca}^{2+}]_i$  buffered to 100 nM with 10 mM EGTA + 3.6 mM  $\text{CaCl}_2$  in the absence (black,  $n=7$ ) or additional presence of 100  $\mu\text{M}$  CaM (blue,  $n=7$ ) in pipette. Application of 5  $\mu\text{M}$  2-APB for 60 s to CaM-treated cells (blue) is indicated in graph. *D*) Average CRAC currents in STIM1+CRACM1 cells induced by 20  $\mu\text{M}$   $\text{InsP}_3$  with  $[\text{Ca}^{2+}]_i$  buffered to 100 nM using 10 mM EGTA + 3.6 mM  $\text{CaCl}_2$ . CRAC currents developed in the absence of added CaM (black,  $n=9$ ) but were rapidly suppressed by 100  $\mu\text{M}$  CaM in pipette (red,  $n=6$ ). Application of 2  $\mu\text{M}$  ionomycin for 3 s (red) reversed the CaM-mediated inhibition of CRAC currents. *E*) Average CRAC current densities in STIM2-expressing HEK293 cells transfected with CRACM1, where  $[\text{Ca}^{2+}]_i$  was clamped to near zero with 20 mM BAPTA. 2-APB (50  $\mu\text{M}$ ) was applied for 30 s as indicated in graph ( $n=7$ ). *F*) Average CRAC current densities at  $-80$  mV in STIM2+CRACM1 cells in response to 20  $\mu\text{M}$   $\text{InsP}_3$  + 20 mM BAPTA. Pipette solution additionally contained 50  $\mu\text{M}$  2-APB. At the indicated time, 50  $\mu\text{M}$  2-APB was applied extracellularly.

filling solution,  $\text{InsP}_3$  induced a sustained CRAC current with monophasic activation kinetics (Fig. 5D, black trace). Addition of 100  $\mu\text{M}$  CaM resulted in a similar activation of CRAC current, but the current was rapidly inactivated (Fig. 5D, red trace). This transient CRAC current response was similar to that observed with STIM2; however, in contrast to STIM2-expressing cells (see Fig. 5B, green trace), subsequent ionomycin application in STIM1-expressing cells completely restored CRAC currents (Fig. 5D, red trace). This result suggests that the CaM-induced inhibition of CRAC currents does not occur at the level of either STIM1 or CRACM1 but instead appears to be mediated by store refilling. Indeed, CaM has been demonstrated to inhibit  $\text{InsP}_3$  receptors (31, 32), and this mechanism would enable stores to refill even in the presence of  $\text{InsP}_3$ . Together, these data suggest that the CaM-mediated inhibition of CRAC currents can occur indirectly through inhibition of  $\text{InsP}_3$  receptors and more directly through inhibition of STIM2-mediated CRAC currents. The latter mechanism is specific for STIM2, since CRAC currents produced through STIM1 remain unaffected by CaM if stores are emptied in an  $\text{InsP}_3$ -independent fashion.

The above data suggest that CaM acts as a specific inhibitor of STIM2 coupled to CRAC channels and dialysis of cells in whole-cell recordings leads to washout of CaM and disinhibition of CRAC channels. By supplementing the pipette solution with CaM, the washout is counteracted and CRAC channels are sup-

pressed; however, 2-APB can still activate the CaM-inhibited channels. A simple interpretation of this result would be that 2-APB might displace the inhibitory CaM from the STIM2/CRACM1 complex. We obtained support for this hypothesis from experiments in which we probed the effects of 2-APB before and after the secondary phase had fully developed. Figure 5E illustrates that the same concentration of 2-APB (50  $\mu\text{M}$ ) produced almost identical peak amplitudes of approximately  $-10$  pA/pF of STIM2-dependent CRAC current when applied 10 s after whole-cell establishment and after the CRAC current reached a plateau, with the second application timed when a significant amount of the endogenous CaM had washed out of the cell. Thus, the absolute efficacy was essentially the same as during the first application, whereas the relative efficacy of the second 2-APB application in facilitating the CRAC current was lower after the inhibitor had washed out when compared to the first application. This result would be compatible with the hypothesis that 2-APB interferes with CaM binding to the STIM2/CRACM1 complex and such a mechanism would presumably occur at an intracellular site. However, we could not obtain direct and conclusive evidence for an intracellular effect of 2-APB. Inclusion of 50  $\mu\text{M}$  2-APB in the patch pipette failed to activate CRAC currents by itself, although  $\text{InsP}_3$ -induced CRAC currents appeared to be delayed and slightly reduced (Fig. 5F). Subsequent extracellular application of 50  $\mu\text{M}$  2-APB, how-

ever, remained fully effective in first facilitating and then blocking CRAC currents. Hence, the exact mechanism and site of action of 2-APB remains to be investigated.

Unlike the situation in whole-cell recordings, the endogenous CaM cannot escape from intact cells, and, therefore, one would expect the initial store-operated activation of CRAC channels by STIM2 to be followed by inhibition, resulting in a transient SOCE phase. We tested this hypothesis in intact cells loaded with the  $\text{Ca}^{2+}$  indicator Fura-2 and stimulated store-operated  $\text{Ca}^{2+}$  influx through muscarinic receptors using carbachol to rapidly deplete stores and thapsigargin to prevent store refilling. This experiment was performed both in the presence and absence of extracellular  $\text{Ca}^{2+}$  and in stable STIM2-expressing HEK293 cells that were transiently transfected with an empty vector or with CRACM1. For comparison, we also included STIM1- and CRACM1-expressing cells. As illustrated in Fig. 6A–C, all cell populations produced a similar transient increase in  $[\text{Ca}^{2+}]_i$  when  $\text{Ca}^{2+}$  was absent, due to  $\text{InsP}_3$ -mediated release of  $\text{Ca}^{2+}$  from intracellular stores. As expected, the presence of extracellular  $\text{Ca}^{2+}$  produced a plateau phase of elevated  $[\text{Ca}^{2+}]_i$  that was likely due to SOCE in all cell populations. However, the CRACM1-expressing cells exhibited a more pronounced shoulder after the release transient due to store-operated activation by STIM1 or STIM2. To better appreciate the differences in  $\text{Ca}^{2+}$  entry between the two populations, we subtracted the signals obtained in the absence of  $\text{Ca}^{2+}$  from those in the presence of  $\text{Ca}^{2+}$  to arrive at the net influx components in the cell populations. As can be seen in Fig. 6D, the STIM1-expressing cells produced a sustained increase in  $[\text{Ca}^{2+}]_i$ , whereas STIM2-expressing cells produced a transient increase in SOCE that decayed. This transient increase in SOCE reflects the SOCE induced by STIM2 coupling to CRACM1 channels after store depletion and presumably the subsequent inhibition by CaM. The slightly increased basal  $[\text{Ca}^{2+}]_i$  of the STIM2- and CRACM1-expressing cells may result from a low level of constitutively open CRAC channels.

## DISCUSSION

Taken together, the above results provide compelling evidence for both store-dependent and store-independent activation of CRAC channels by STIM2. Our data suggest that in stably transfected HEK293 cells, STIM2 exists in at least two functional states, with most of the STIM2 molecules coupling to CRAC channels in a store-independent manner (constitutively coupled) and a smaller population of STIM2 molecules remaining available to activate CRAC channels after store depletion (store coupled). Store-dependent activation can be demonstrated both in patch-clamp experiments when cells are perfused with  $\text{InsP}_3$  (Fig. 3A) or when store depletion is caused by ionomycin (Fig. 3C), which both result in rapid activation of CRAC currents. SOCE is also evident in  $[\text{Ca}^{2+}]_i$  imaging experiments in intact cells when cells are stimulated with an  $\text{InsP}_3$ -mobilizing agonist and blocking store refilling with thapsigargin (Fig. 6). The main difference between CRAC in patch-clamp experiments and SOCE in intact cells is that the latter manifests itself as a transient increase in  $[\text{Ca}^{2+}]_i$  (Fig. 6), whereas whole-cell recordings exhibit a more persistent CRAC current that is followed by an even larger, secondary activation of CRAC channel activity (Fig. 3A, C, F). The transient nature of STIM2-mediated SOCE in intact cells may also explain why the store-operated mechanism remained undetected in typical assays of SOCE (14, 16), where thapsigargin-induced store depletion in zero extracellular  $\text{Ca}^{2+}$  is followed by  $\text{Ca}^{2+}$  readmission after several hundreds of seconds to probe SOCE. During the thapsigargin/zero  $\text{Ca}^{2+}$  exposure, any STIM2-mediated SOCE would remain undetectable and channel activity would have subsided by the time  $\text{Ca}^{2+}$  is readmitted.

The second population of STIM2 molecules is not coupled to store depletion (14). It is observed in patch-clamp experiments as a large CRAC current that typically activates after  $\sim 100$ – $200$  s under a variety of experimental conditions, regardless of the filling state of intracellular stores. Although the store-operated population can be suppressed experimentally in maintaining the stores filled with  $\text{Ca}^{2+}$ , the store-independent population can only be delayed by reducing the

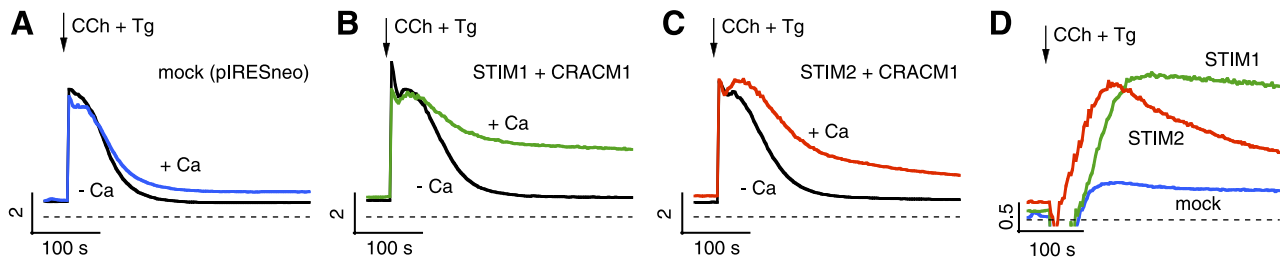


**Figure 6.** STIM2 causes transient SOCE in intact cells. *A*) Changes in  $[\text{Ca}^{2+}]_i$  measured as ratios of fura-2 fluorescence excited at 340 and 380 nm in STIM2 cells transfected with empty vector in the absence (black) or presence (blue) of 1 mM extracellular  $\text{Ca}^{2+}$ . Carbachol (100  $\mu\text{M}$ ) and thapsigargin (2  $\mu\text{M}$ ) were applied as indicated by arrow and maintained for duration of experiment. *B*) Identical experimental conditions as in *A*, but for STIM1 + CRACM1 cells. *C*) Identical experimental conditions as in *A*, but for STIM2 + CRACM1 cells. *D*) These traces represent subtracted traces from *A*–*C*, where  $[\text{Ca}^{2+}]_i$  signal in  $\text{Ca}^{2+}$ -free solution was subtracted from that obtained with  $\text{Ca}^{2+}$  to yield net  $\text{Ca}^{2+}$  entry.

rate of diffusion through the pipette and the cytosol (Fig. 5A), which effectively slows down the washout and loss of a cytosolic factor that normally inhibits the constitutive activity of STIM2 and CRACM1. We propose that this cytosolic factor is CaM, since inclusion of CaM in the pipette filling solution completely suppresses activation of the slow CRAC current phase (Fig. 5B). This inhibition requires at least resting levels of  $[Ca^{2+}]_i$  approximately  $\sim 100$  nM, as apo-CaM is ineffective when  $[Ca^{2+}]_i$  is buffered to near zero (Fig. 5B). In the case of store-operated activation of CRACM1 by STIM2, we surmise that the CaM is initially absent, so activation can take place. Subsequently, possibly mediated by the increase in  $[Ca^{2+}]_{ii}$ ,  $Ca^{2+}$ -CaM is recruited to the STIM2/CRACM1 complex and inhibits channel activity to cause transient SOCE. In addition, CaM appears to also have a more general effect on SOCE that is mediated through inhibition of  $InsP_3$  receptor activity (31, 32). This effect allows stores to refill even in the presence of high levels of  $InsP_3$  and results in suppression of CRAC channel activity independently of whether CRAC channels are activated through STIM1 or STIM2. Sidestepping this  $InsP_3$ -dependent regulation by enforcing store depletion through ionomycin reveals that the inhibitory effect of CaM at the STIM/CRAC complex is specific to STIM2, as it is not observed with STIM1 (Fig. 5C, D).

Similar to CaM, G418 appears to be an effective and potent inhibitor of STIM2-mediated CRAC channel activation. In cells grown in the presence of G418, both populations of STIM2 molecules are blocked by the antibiotic at the intracellular side (Fig. 4A, B). An attractive hypothesis that remains to be substantiated would be that G418 acts as a CaM mimetic and occupies the same inhibitory binding site as CaM on the STIM2/CRACM1 complexes. Consistent with this notion is the finding that regardless of whether the STIM2/CRACM1 complexes are suppressed by G418 or the endogenous CaM, they can be rapidly activated by 2-APB. This activation is so rapid that it cannot possibly result from store depletion. The fastest store-dependent activation of CRAC currents by  $InsP_3$  is typically characterized by  $\sim 4$ – $6$  s delay and then proceeds over  $\sim 60$  s to reach full activation. However, the 2-APB-mediated activation occurs with a half-time of  $\sim 2$  s and is virtually complete within 5 s (Fig. 1E, F), *i.e.*, at a time when store-dependent activation just begins. This rapid, store-independent gating of CRAC channels appears to be mediated by some close interaction of STIM2 and CRACM1, as it is not observed in cells overexpressing CRACM1 alone or in combination with STIM1. It is tempting to speculate that agonist-mediated signals might recruit these precoupled STIM2/CRAC complexes to activate CRAC channels even without store depletion and with very fast kinetics. In this context, we note that the carbachol-induced activation of  $Ca^{2+}$  influx illustrated in Fig. 6 develops considerably more quickly in STIM2-expressing cells than in STIM1 expressors (see Fig. 6D).

At this point, it remains unclear how 2-APB can achieve such fast gating of CRAC channels and even overcome the apparent block by G418 and CaM. If we accept that STIM2 activates CRACM1 *via* direct binding in a conformational coupling manner, the simplest interpretation would be that 2-APB simply displaces G418 or CaM from its binding site on the STIM2/CRACM1 complex. This would imply an intracellular action 2-APB; however, this issue remains unresolved, since both facilitatory and inhibitory effects of 2-APB are only seen when the compound is applied extracellularly (26). We confirmed that intracellularly applied 2-APB (50  $\mu$ M) is indeed ineffective in activating or suppressing CRAC currents, whereas subsequent extracellular application of 50  $\mu$ M 2-APB first activates and then inhibits CRAC currents (Fig. 5F). However, lipophilic compounds are often ineffective when applied intracellularly in patch-clamp experiments and extracellularly applied 2-APB has been demonstrated to be membrane permeable and suppress  $InsP_3$  receptor function (33), suggesting that, in principle, the compound might gain access to the cytosol when applied extracellularly.

Taken together, our data provide compelling evidence for a bimodal functional coupling between STIM2 to CRACM channels, with both store-dependent and -independent components. Since both STIM1 and STIM2 are widely expressed (34), both may serve distinct, but important, roles in SOCE. Relative differences in ER  $Ca^{2+}$  sensing by the two proteins may provide a broader sensitivity to store emptying. STIM2 is additionally activable in a store-independent manner, with the rapid action of 2-APB revealing that a substantial component of STIM2 appears to be in a precoupled configuration. Identifying physiological mechanisms that regulate this process would be an important future area of investigation. Indeed, the revelation that both components of STIM2-mediated channel activation are modified by CaM provides an important clue to the role of a potentially powerful cytosolic  $Ca^{2+}$ -mediated control process in the activation of CRAC channels, complementing the clear role of luminal  $Ca^{2+}$  in activating the channels. EJ

We thank M. Bellinger and A. Love for help with cell culture and transfections. Supported in part by National Institutes of Health (NIH) grants R01-AI050200 and R01-NS040927 (R.P.) and AI058173 (D.L.G.). C.P. was supported by a fellowship from the Deutsche Forschungsgemeinschaft (PE-1478/1-1).

## REFERENCES

1. Parekh, A. B., and Penner, R. (1997) Store depletion and calcium influx. *Physiol. Rev.* **77**, 901–930
2. Parekh, A. B., and Putney, J. W., Jr. (2005) Store-operated calcium channels. *Physiol. Rev.* **85**, 757–810
3. Putney, J. W., Jr. (1990) Capacitative calcium entry revisited. *Cell Calcium* **11**, 611–624
4. Hoth, M., and Penner, R. (1993) Calcium release-activated calcium current in rat mast cells. *J. Physiol.* **465**, 359–386

5. Hoth, M., and Penner, R. (1992) Depletion of intracellular calcium stores activates a calcium current in mast cells. *Nature* **355**, 353–356
6. Zweifach, A., and Lewis, R. S. (1993) Mitogen-regulated  $\text{Ca}^{2+}$  current of T lymphocytes is activated by depletion of intracellular  $\text{Ca}^{2+}$  stores. *Proc. Natl. Acad. Sci. U. S. A.* **90**, 6295–6299
7. Feske, S., Gwack, Y., Prakriya, M., Srikanth, S., Puppel, S. H., Tanasa, B., Hogan, P. G., Lewis, R. S., Daly, M., and Rao, A. (2006) A mutation in Orai1 causes immune deficiency by abrogating CRAC channel function. *Nature* **441**, 179–185
8. Liou, J., Kim, M. L., Heo, W. D., Jones, J. T., Myers, J. W., Ferrell, J. E., Jr., and Meyer, T. (2005) STIM is a  $\text{Ca}^{2+}$  sensor essential for  $\text{Ca}^{2+}$ -store-depletion-triggered  $\text{Ca}^{2+}$  influx. *Curr. Biol.* **15**, 1235–1241
9. Roos, J., DiGregorio, P. J., Yeromin, A. V., Ohlsen, K., Lioudyno, M., Zhang, S., Safrina, O., Kozak, J. A., Wagner, S. L., Cahalan, M. D., Velicelbi, G., and Stauderman, K. A. (2005) STIM1, an essential and conserved component of store-operated  $\text{Ca}^{2+}$  channel function. *J. Cell Biol.* **169**, 435–445
10. Vig, M., Peinelt, C., Beck, A., Koomoa, D. L., Rabah, D., Koblan-Huberson, M., Kraft, S., Turner, H., Fleig, A., Penner, R., and Kinet, J. P. (2006) CRACM1 is a plasma membrane protein essential for store-operated  $\text{Ca}^{2+}$  entry. *Science* **312**, 1220–1223
11. Zhang, S. L., Yeromin, A. V., Zhang, X. H., Yu, Y., Safrina, O., Penna, A., Roos, J., Stauderman, K. A., and Cahalan, M. D. (2006) Genome-wide RNAi screen of  $\text{Ca}^{2+}$  influx identifies genes that regulate  $\text{Ca}^{2+}$  release-activated  $\text{Ca}^{2+}$  channel activity. *Proc. Natl. Acad. Sci. U. S. A.* **103**, 9357–9362
12. Mercer, J. C., Dehaven, W. I., Smyth, J. T., Wedel, B., Boyles, R. R., Bird, G. S., and Putney, J. W., Jr. (2006) Large store-operated calcium selective currents due to co-expression of Orai1 or Orai2 with the intracellular calcium sensor, Stim1. *J. Biol. Chem.* **281**, 24979–24990
13. Peinelt, C., Vig, M., Koomoa, D. L., Beck, A., Nadler, M. J., Koblan-Huberson, M., Lis, A., Fleig, A., Penner, R., and Kinet, J. P. (2006) Amplification of CRAC current by STIM1 and CRACM1 (Orai1). *Nat. Cell Biol.* **8**, 771–773
14. Soboloff, J., Spassova, M. A., Tang, X. D., Hewavitharana, T., Xu, W., and Gill, D. L. (2006) Orai1 and STIM reconstitute store-operated calcium channel function. *J. Biol. Chem.* **281**, 20661–20665
15. Wu, M. M., Buchanan, J., Luik, R. M., and Lewis, R. S. (2006)  $\text{Ca}^{2+}$  store depletion causes STIM1 to accumulate in ER regions closely associated with the plasma membrane. *J. Cell Biol.* **174**, 803–813
16. Soboloff, J., Spassova, M. A., Hewavitharana, T., He, L. P., Xu, W., Johnstone, L. S., Dziadek, M. A., and Gill, D. L. (2006) STIM2 is an inhibitor of STIM1-mediated store-operated  $\text{Ca}^{2+}$  entry. *Curr. Biol.* **16**, 1465–1470
17. Zhang, S. L., Yu, Y., Roos, J., Kozak, J. A., Deerinck, T. J., Ellisman, M. H., Stauderman, K. A., and Cahalan, M. D. (2005) STIM1 is a  $\text{Ca}^{2+}$  sensor that activates CRAC channels and migrates from the  $\text{Ca}^{2+}$  store to the plasma membrane. *Nature* **437**, 902–905
18. Vig, M., Beck, A., Billingsley, J. M., Lis, A., Parvez, S., Peinelt, C., Koomoa, D. L., Soboloff, J., Gill, D. L., Fleig, A., Kinet, J. P., and Penner, R. (2006) CRACM1 multimers form the ion-selective pore of the CRAC channel. *Curr. Biol.* **16**, 2073–2079
19. Yeromin, A. V., Zhang, S. L., Jiang, W., Yu, Y., Safrina, O., and Cahalan, M. D. (2006) Molecular identification of the CRAC channel by altered ion selectivity in a mutant of Orai. *Nature* **443**, 226–229
20. Prakriya, M., Feske, S., Gwack, Y., Srikanth, S., Rao, A., and Hogan, P. G. (2006) Orai1 is an essential pore subunit of the CRAC channel. *Nature* **443**, 230–233
21. Gwack, Y., Srikanth, S., Feske, S., Cruz-Guilloty, F., Oh-Hora, M., Neems, D. S., Hogan, P. G., and Rao, A. (2007) Biochemical and functional characterization of Orai family proteins. *J. Biol. Chem.* **282**, 16232–16243
22. Lis, A., Peinelt, C., Beck, A., Parvez, S., Monteilh-Zoller, M., Fleig, A., and Penner, R. (2007) CRACM1, CRACM2, and CRACM3 are store-operated  $\text{Ca}^{2+}$  channels with distinct functional properties. *Curr. Biol.* **17**, 794–800
23. Ma, H. T., Venkatachalam, K., Parys, J. B., and Gill, D. L. (2002) Modification of store-operated channel coupling and inositol trisphosphate receptor function by 2-aminoethoxydiphenyl borate in DT40 lymphocytes. *J. Biol. Chem.* **277**, 6915–6922
24. Braun, F. J., Broad, L. M., Armstrong, D. L., and Putney, J. W., Jr. (2001) Stable activation of single  $\text{Ca}^{2+}$  release-activated  $\text{Ca}^{2+}$  channels in divalent cation-free solutions. *J. Biol. Chem.* **276**, 10633–1070
25. Hermosura, M. C., Monteilh-Zoller, M. K., Scharenberg, A. M., Penner, R., and Fleig, A. (2002) Dissociation of the store-operated calcium current  $I_{\text{CRAC}}$  and the Mg-nucleotide-regulated metal ion current  $\text{MgNuM}$ . *J. Physiol.* **539**, 445–458
26. Prakriya, M., and Lewis, R. S. (2001) Potentiation and inhibition of  $\text{Ca}^{2+}$  release-activated  $\text{Ca}^{2+}$  channels by 2-aminoethylidiphenyl borate (2-APB) occurs independently of  $\text{IP}_3$  receptors. *J. Physiol.* **536**, 3–19
27. Spassova, M. A., Soboloff, J., He, L. P., Xu, W., Dziadek, M. A., and Gill, D. L. (2006) STIM1 has a plasma membrane role in the activation of store-operated  $\text{Ca}^{2+}$  channels. *Proc. Natl. Acad. Sci. U. S. A.* **103**, 4040–4045
28. Levitan, I. B. (1999) It is calmodulin after all! Mediator of the calcium modulation of multiple ion channels. *Neuron* **22**, 645–648
29. Moreau, B., Straube, S., Fisher, R. J., Putney, J. W., Jr., and Parekh, A. B. (2005)  $\text{Ca}^{2+}$ -calmodulin-dependent facilitation and  $\text{Ca}^{2+}$  inactivation of  $\text{Ca}^{2+}$  release-activated  $\text{Ca}^{2+}$  channels. *J. Biol. Chem.* **280**, 8776–8783
30. Vaca, L. (1996) Calmodulin inhibits calcium influx current in vascular endothelium. *FEBS Lett.* **390**, 289–293
31. Adkins, C. E., Morris, S. A., De Smedt, H., Sienaert, I., Torok, K., and Taylor, C. W. (2000)  $\text{Ca}^{2+}$ -calmodulin inhibits  $\text{Ca}^{2+}$  release mediated by type-1, -2 and -3 inositol trisphosphate receptors. *Biochem. J.* **345**, Pt. 2, 357–363
32. Patel, S., Morris, S. A., Adkins, C. E., O’Beirne, G., and Taylor, C. W. (1997)  $\text{Ca}^{2+}$ -independent inhibition of inositol trisphosphate receptors by calmodulin: redistribution of calmodulin as a possible means of regulating  $\text{Ca}^{2+}$  mobilization. *Proc. Natl. Acad. Sci. U. S. A.* **94**, 11627–11632
33. Maruyama, T., Kanaji, T., Nakade, S., Kanno, T., and Mikoshiba, K. (1997) 2APB, 2-aminoethoxydiphenyl borate, a membrane-penetrable modulator of  $\text{Ins}(1,4,5)\text{P}_3$ -induced  $\text{Ca}^{2+}$  release. *J. Biochem.* **122**, 498–505
34. Williams, R. T., Manji, S. S., Parker, N. J., Hancock, M. S., Van Stekelenburg, L., Eid, J. P., Senior, P. V., Kazenwadel, J. S., Shandala, T., Saint, R., Smith, P. J., and Dziadek, M. A. (2001) Identification and characterization of the STIM (stromal interaction molecule) gene family: coding for a novel class of transmembrane proteins. *Biochem. J.* **357**, 673–685

Received for publication July 22, 2007.  
Accepted for publication August 30, 2007.